Conformational analysis and vibrational spectroscopic investigation of L-proline-tyrosine (L-Pro-Tyr) dipeptide

ARTICLE *in* JOURNAL OF MOLECULAR STRUCTURE · MAY 2011

Impact Factor: 1.6 · DOI: 10.1016/j.molstruc.2011.01.030

5 AUTHORS, INCLUDING:

Serda Kecel Gunduz
Istanbul University
13 PUBLICATIONS **56** CITATIONS
SEE PROFILE

Sevim Akyuz
T.C. Istanbul Kultur University
170 PUBLICATIONS **1,524** CITATIONS
SEE PROFILE

Sefa Celik
Istanbul University
13 PUBLICATIONS **48** CITATIONS
SEE PROFILE

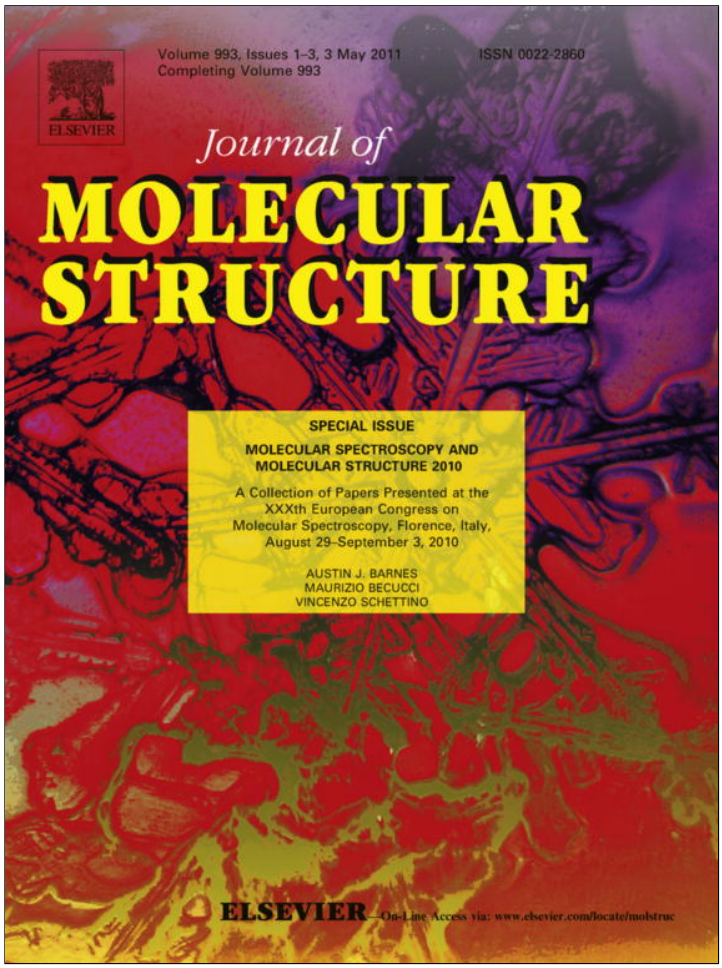

Journal of Molecular Structure 993 (2011) 349–356

Contents lists available at ScienceDirect

Journal of Molecular Structure

journal homepage: www.elsevier.com/locate/molstruc

Conformational analysis and vibrational spectroscopic investigation of L-proline–tyrosine (L-Pro–Tyr) dipeptide

Serda Kecel [a], Aysen E. Ozel [a,*], Sevim Akyuz [b], Sefa Celik [c], Gulshen Agaeva [d]

[a] Istanbul University, Faculty of Science, Department of Physics, Vezneciler, 34134 Istanbul, Turkey
[b] Istanbul Kultur University, Faculty of Science and Letters, Department of Physics, Atakoy Campus, 34156 Istanbul, Turkey
[c] Istanbul University, Engineering Faculty, Electrical-Electronics Eng. Department, 34320 Avcilar, Istanbul, Turkey
[d] Institute of Physical Problems, Baku State University, AZ-1148 Baku, Azerbaijan

ARTICLE INFO

Article history:
Available online 23 January 2011

Keywords:
Conformational analysis
Density functional theory
Dipeptide
IR and Raman spectra
Proline
Tyrosine

ABSTRACT

In this study the conformational properties of the drug based dipeptide L-proline–L-tyrosine (Pro–Tyr) in its monomeric and dimeric forms, have been investigated by molecular mechanic and ab initio calculations. The energy calculations on Pro–Tyr dipeptide as a function of side chains torsion angles, enable us to determine their energetically preferred conformations. One-hundred and eight possible conformations of Pro–Tyr dipeptide have been investigated by conformational analysis and the low energy conformations of dipeptide have been determined by using the Ramachandran maps. Afterwards, the geometrical parameters of obtained stable conformations were used as starting parameters for quantum chemical calculations. The molecular structure of Pro–Tyr dipeptide, in the ground electronic state (in vacuum) was optimized by density functional theory method with B3LYP functional and using 6-31G(d,p) and 6-31++G(d,p) basis sets. The dimeric forms of the dipeptide were also formed and energetically preferred conformations of dimers were investigated using the same method and the same level of theory by using 6-31G(d,p) basic set. The fundamental vibrational wavenumbers, IR intensities and Raman activities of the global conformation of monomeric and dimeric forms of the dipeptide were calculated and compared with the experimental vibrational spectra of solid Pro–Tyr dipeptide. The total energy distributions (TED) of the vibrational modes were calculated by using Scaled Quantum Mechanical (SQM) analysis. Vibrational assignment was performed on the basis of calculated total energy distribution (TED) of the modes.

1. Introduction

Tyrosine is a non-essential amino acid which is found in almost all proteins in the body. It helps to regulate mood, stimulates the nervous system and support the formation of neurotransmitters including dopamine, norepinephrine and epinephrine. Tyrosine is involved in the synthesis of melanin which protects against the harmful effects of ultraviolet light [1] and, also been used for treatment of allergies, headaches and Parkinson's disease. Tyrosine is needed for normal functioning of the thyroid, pituitary, and adrenal glands. On the other hand proline is an amino acid which is needed for the production of collagen and cartilage, which are important for the formation of bone. It keeps muscles and joints flexible and helps reduce sagging and wrinkling. Pro–Tyr–NH_2 dipeptide is the simplest peptide analogs of sulpiride [2], which has antipsychotic properties. Despite of biological importance, to the best of our knowledge, no conformational analysis, or ab initio, DFT calculations have been reported yet for Pro–Tyr dipeptide, although there are a number of studies on tyrosine [3–5] and proline [6–13] amino acids. Proline mono peptide has particular rigid structure [6–13]; it has an imino group is fixed within a pyrrolidine ring, which makes proline conformationally less flexible, in comparison with most other amino acids. The conformational behavior of proline in the Pro–Tyr dipeptide, therefore, is thought to be interesting. Besides, the determination of conformational possibilities of L-Pro–Tyr dipeptide may be useful as a base for synthesis of its more effective structural analogs. In this study, conformational analysis, theoretical and experimental vibrational spectra of Pro–Tyr dipeptide in its monomeric and dimeric forms are reported for the first time.

2. Experimental and computational details

The Pro–Tyr dipeptide was purchased from GL-biochem Ltd., and used as received. The FT-IR spectrum of KBr disk of the dipeptide was recorded on a Jasco 300E FT-IR spectrometer in the range 400–4000 cm^{-1} with a resolution of 2 cm^{-1} based on averaging 200 sample and 30 background scans. The Raman spectrum of the sample was taken with a Jasco NRS-3100 micro Raman

* Corresponding author.
E-mail address: aozel@istanbul.edu.tr (A.E. Ozel).

0022-2860/$ - see front matter © 2011 Elsevier B.V. All rights reserved.
doi:10.1016/j.molstruc.2011.01.030

spectrometer (1800 lines/mm or 1200 lines/mm grating and high sensitivity cooled CCD). Sample was excited with a 531.96 nm diode laser. The Raman system was calibrated with a silicon semiconductor using the Raman peak at 520 cm^{-1}. A 20× microscope objective (Olympus) was used to focus the laser and collect Raman scattering on the sample. Spectral resolution was 3.9 cm^{-1} and 100 spectra were accumulated.

The conformational analysis was carried out by sequential method with combining all low energy conformations of constitutive residues and by using a program proposed by Godjaev et al. [14]. The low energy conformations of dipeptide have been determined by using the Ramachandran maps [15,16]. All the ab initio calculations are performed by using Gaussian 03 program [17] package. Due to success in calculating the electronic structure and energy, the calculations were carried out by using the hybrid density functional theory (DFT/B3LYP) method. For monomeric calculations both 6-31G(d,p) and 6-31++G(d,p) basic sets and for dimeric calculations only 6-31G(d,p) basis set were used. We could not use 6-31++G(d,p) basic set for the dimeric form due to inadequate capacity of our computer.

The total energy distribution (TED) of the vibrational modes of the molecules was calculated with the Scaled Quantum Mechanics (SQM) method by using the Parallel Quantum Mechanics Solutions (PQS) program [18].

3. Results and discussion

The Pro–Tyr dipeptide ($C_{14}H_{18}N_2O_4$) consists of 38 atoms, accordingly has 108 vibrational modes. The molecular model of the Pro–Tyr dipeptide is given in Fig. 1a.

In the first part of this study, the theoretical conformational analysis on Pro–Tyr dipeptide was carried out in order to determine its energetically preferred conformers. The stable conformations of the Pro–Tyr dipeptide were calculated by examination of all possible combinations of the local minima of the two amino acid residues. The starting structural approximations for this dipeptide were chosen with regard to the limitations associated with the Pro residue. The global conformation of Pro–Tyr dipeptide has been determined by using Ramachandran maps [15,16]. These maps have four regions (B, R, L and P) and the backbone rotations are characterized with φ and Ψ angles which values are restricted between +180° and −180°; B(φ = −180–0°, Ψ = 0–180°), R(φ, Ψ = −180–0°), L(φ, Ψ = 0–180°) and P(φ = 0–180°, Ψ = −180–0°). On the other hand, rotations of the side chains are determined with χ angles [19]. The possible extended or folded backbone conformations are named shape. The dipeptide shape is divided into two forms; folded (f) and extended (e). RR, RB, BP, LL, LP, LR, PB and BL forms produce (f) shape and BB, BR, RL, LB, LR, RP, PL and PP forms produce (e) shape of the dipeptides. In Fig. 1a, the backbone and the side chains angles of Pro–Tyr dipeptide, together with the atom numbering, used in DFT calculations, were given.

For Pro–Tyr dipeptide, the values of dihedral angles were taken from the B and R areas for proline and the B, R and L areas for the tyrosine. The values of dihedral angles of the side chains $\chi^1$and χ^2 were taken to be 60°, 180°, −60° and 90°, −90° respectively (see Fig. 1). The angle χ^3 of Tyr was taken as equal to 180°.

We examined 108 conformers for mono-L-Pro–Tyr dipeptide. The global conformation of the mono L-Pro–Tyr dipeptide is characterized by the folded backbone shape in the RR conformational range, with −7.14 kcal/mol energy. The conformational energy of mono-L-Pro–Tyr molecule (E_{tot} = −7.14 kcal/mol) was found as the sum of the van der Waals (E_{vdW} = −5.74 kcal/mol), electrostatic (E_{el} = −1.57 kcal/mol), torsional (E_{tor} = 0.17 kcal/mol) energies. The optimized values of the dihedral angles of backbone and side chains of the Pro–Tyr dipeptide are found to be; Ψ_1 = −52.37, ω = 179.40, φ = −139.83, χ_{21} = −57.13, χ_{22} = 101.32, χ_{23} = 179.82, Ψ_2 = −60.00.

In the second part of this study, the geometry optimization of the obtained global conformation was performed by DFT/B3LYP method by using both 6-31G(d,p) and 6-31++G(d,p) basis sets, and after then the vibrational wavenumbers were calculated. The same calculations were repeated for the dimeric form of the dipeptide, but, only by using 6-31G(d,p) basis set.

The molecular structure of the neutral monomeric and dimeric forms of L-Pro–Tyr with the atom numbering and the optimized dihedral angles are shown in Fig. 1. Calculated bond distances, interbond angles and torsion angles of monomeric (for both 6-31G(d,p) and 6-31++(G(d,p) basic sets) and dimeric forms (6-31G(d,p)) of Pro–Tyr dipeptide are tabulated in Table 1. We could not use 6-31++G(d,p) basis set for the dimeric form of Pro–Tyr dipeptide due to inadequate capacity of our computer. However, as seen in Table 1, considerable changes were not obtained using 6-31++G(d,p) basic set instead of 6-31G(d,p), in the monomeric form of Pro–Tyr dipeptide. As a result, we compared calculation results with 6-31G(d,p) basis set of monomeric form to those of dimeric form.

Two possible intra H-bonding interactions between H(17) and O(36) (2.60 Å), N(2) and H(17)(2.13 Å) were predicted for the global conformation of monomeric L-Pro–Tyr dipeptide.

L-Pro–Tyr dipeptide has applicable geometry to constitute a dimeric form due to its carboxyl groups. The dimeric forms of the

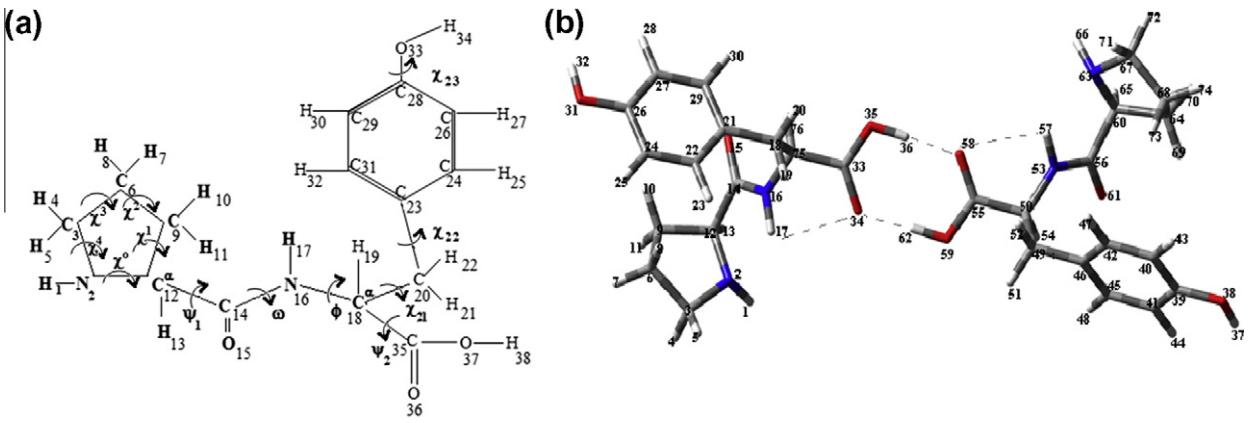

Fig. 1. The molecular model of neutral L-Pro–Tyr dipeptide (a). Atom numbering and dihedral angles were shown. The global conformation of dimeric form of Pro–Tyr dipeptide (b). Predicted H-bonding interactions are shown as broken lines.

Table 1
The geometry of monomeric and dimeric forms of Pro–Tyr dipeptide, calculated at the DFT level of theory using 6-31G(d,p) and 6-31G++(d,p) basis sets. (distance in Å, angles in °).

Bond	Mono		Dimer	Angle	Mono		Dimer	Dihedral	Mono		Dimer
	6-31G(d,p)	6-31G++(d,p)	6-31G(d,p)		6-31G(d,p)	6-31G ++(d,p)	6-31G(d,p)		6-31G(d,p)	6-31G++(d,p)	6-31G(d,p)
R(1.2)	1.0135	1.0141	1.0136	A(2.3.6)	103.4403	103.1730	103.3392	D(1.2.3.4)	−32.6154	−35.8088	−33.5364
R(2.3)	1.4768	1.4776	1.4764	**A(2.12.9)**	**105.5307**	**105.3562**	**105.4970**	D(1.2.3.5)	87.5903	84.5917	86.7164
R(2.12)	1.4803	1.4800	1.4800	A(3.2.12)	109.4762	109.6360	109.4590	D(1.2.12.14)	−111.1078	−105.9708	−109.8387
R(3.4)	1.102	1.1021	1.1021	A(3.6.7)	112.5727	112.5425	112.5871	D(15.14.16.17)	−173.974	−174.5389	−174.8824
R(3.5)	1.0957	1.0954	1.0957	A(3.6.8)	110.2857	110.2140	110.2500	**D(14.16.18.17)**	**−168.8723**	**−168.8375**	**−170.7497**
R(3.6)	1.5322	1.5323	1.5322	A(3.6.9)	102.3557	102.5039	102.3160	**D(12.14.16.15)**	**−179.6339**	**−179.7818**	**−179.6076**
R(6.7)	1.0934	1.0939	1.0933	A(4.3.5)	107.5489	107.8592	107.5659	**D(12.14.16.18)**	**175.8820**	**175.17946**	**176.7889**
R(6.8)	1.0953	1.0957	1.0952	A(4.3.6)	109.8918	109.9900	109.9066	**D(12.14.16.17)**	**−2.9029**	**−2.5991**	**−2.4990**
R(6.9)	1.536	1.5382	1.5363	A(5.3.6)	113.0494	113.1754	113.0799	**D(14.16.18.35)**	**−123.4513**	**−107.7061**	**−125.2795**
R(9.10)	1.0956	1.0955	1.0955	**A(9.12.13)**	**110.4822**	**110.2041**	**110.3562**	D(16.18.35.36)	−16.8419	−20.9436	−18.2597
R(9.11)	1.0915	1.092	1.0914	**A(9.12.14)**	**110.9807**	**111.6618**	**111.0720**	D(16.18.35.37)	165.4208	161.1404	164.2034
R(9.12)	1.5491	1.5527	1.5500	**A(12.14.15)**	**120.9409**	**120.735**	**120.9188**	D(18.35.37.38)	177.5184	177.8544	177.0852
R(12.13)	1.0965	1.0969	1.0966	**A(12.14.16)**	**114.5295**	**114.9947**	**114.6026**	D(19.18.35.36)	−133.2958	−137.5852	−134.8857
R(12.14)	**1.5406**	**1.5393**	**1.5399**	**A(14.16.17)**	**115.5197**	**114.9979**	**115.6383**	D(19.18.35.37)	48.9668	44.4989	47.5774
R(14.15)	**1.2282**	**1.2312**	**1.2285**	**A(14.16.18)**	**122.1458**	**122.6962**	**122.0156**	D(20.18.35.36)	107.9152	103.4515	106.8370
R(14.16)	**1.3587**	**1.3591**	**1.3585**	**A(15.14.16)**	**124.5286**	**124.2699**	**124.4774**	D(20.18.35.37)	−69.8221	−74.4644	−70.6997
R(16.17)	**1.0157**	**1.0166**	**1.0155**	**A(17.16.18)**	**121.4693**	**121.4441**	**121.7486**	D(36.35.37.38)	−0.2886	−0.1360	−0.3844
R(16.18)	**1.4394**	**1.4406**	**1.4394**	**A(20.18.16)**	**113.2266**	**112.5267**	**113.3188**				
R(18.19)	1.0945	1.094	1.0966	**A(20.18.19)**	**108.9318**	**109.4475**	**108.9005**				
R(18.20)	1.5594	1.5569	1.5126	**A(20.18.35)**	**109.1702**	**109.1959**	**108.7564**				
R(26.27)	1.0849	1.0852	1.0849	A(35.37.38)	106.3192	107.3415	110.5060				
R(26.28)	1.3976	1.3973	1.3674	A(36.35.37)	122.9100	122.7527	124.5590				

dipeptide were constructed by bringing together two identical L-Pro–Tyr monomers in global conformation (see Fig. 1b). The calculation, performed by DFT/B3LYP method with the 6-31G(d,p) basis set, predicted intra H bonds of dimeric form between H(17) and O(34) (2.56 Å), H(57) and O(58) (2.56 Å). The inter H bonds of dimeric form were established between mutual carboxyl groups; between O(36) and H(58) (1.63 Å), O(34) and H(62) (1.63 Å).

In order to investigate the geometry around α-carbon atom, the dihedral angles of the amide plane, the bond angles and the bond lengths of the amide plane in dipeptide structure were examined. The 12C and 18C are the α-carbon atoms for monomeric form of Pro–Tyr dipeptide. Five bond lengths (in Å) for the amide planes, considered are 12C–14C, 14C–15O, 14C–16N, 16N–18C and 16N–17H (see Table 1). The peptide bond of Phe–Tyr and Val–Tyr dipeptides were found to be 1.367 Å [20] and 1.366 Å [21], respectively. In this study, this bond length was estimated to be 1.358 Å for monomeric form of Pro–Tyr dipeptide.

The six bond angles (in °) related to amide plane were investigated; those are ∠CCO (12,14,15), ∠ CCN (12,14,16), ∠ OCN (15,14,16), ∠ CNC (14,16,18), ∠ CNH (14,16,17) and ∠ HNC (17,16,18), their computed values were listed in Table 1, as bold. The geometry of α-carbon atom influences the secondary structure of dipeptide. The expected value of bond angle around carbon atom is 109.5°. But due to the streogenic nature of α-carbon atom, the ideal value is not nature. Two α-C centers are 12C and 18C for monomer Pro–Tyr, and investigated α-carbon atom bond angles are ∠CCαN (9,12,2), ∠CCαH (9,12,13), ∠CCα plane (9,12,14), ∠RCαC (20,18,35), ∠RCαH (20,18,19) and ∠RCα plane (20,18,16). Their computed values are 105.5307°, 110.4822°, 110.9807°, 109.1702°, 108.9318° and 113.2266° respectively.

To investigate of the peptide molecules, planarity of the amide plane and knowledge of the peptide bond are very important. The analysis of dihedral angles explains deviations from planarity. The first dihedral angle between atoms 18C and 17H with respect to atoms 14C and 16N (peptide bond is 14C and 16N) is important for amide plane, it should be 180° if the amide plane is planar. The second dihedral angle is between 16N and 15O with respect to the bond joining atoms 12C and 14C. The third dihedral angle is between 12C and 18C with respect to the peptide bond and the fourth dihedral angle is between 12C and 17H with respect to the peptide bond. For planarity dihedral angles should be 180°, 180°, 180° and 0° respectively [20]. In this work calculated dihedral values are, −168.87°, −179.63°, 175.88° and −2.90°. It is clear that Pro–Tyr dipeptide gives non-planar structure of the amide plane. Deviation of first dihedral angle from planarity is ≈−11.13°. Due to H-bonding between amide plane hydrogen 17H and 36O (∼2.60 Å) of carboxylic group of dipeptide, stronger deviation of dihedral angle from 180° were occured. As the interatomic distance is appropriate for hydrogen bonding and the steric interference between N-terminus and R-group in peptide system, the dihedral angles tend to deviation from 180°.

Φ is the dihedral angle between atom 14C and 35C about 16N–18C bond. The computed value of the Φ dihedral angle is −123.45° for monomeric form of Pro–Tyr. The Φ dihedral was found to be −113.96° for Phe–Tyr [20] and −148.53° for Val–Tyr dipeptides [21].

Since proline is a unique in that its side chain is covalently bonded to the nitrogen atom of the peptide backbone, it is found to be interesting to compare conformational behavior of proline in Pro–Tyr dipeptide with those of L-proline monomer [6,7,12,13,22]. Table 2 shows our conformational analysis and DFT calculation results of proline, in comparison to those of relevant data [6,7,12,13]. As aforementioned, the conformational analysis results were used as initial geometric parameters for DFT calculations. Several statistical and energetic studies have shown

Table 2
Pyrrolidine ring structure of proline in Pro–Tyr dipeptide calculated by conformational analysis (conf. Anal.) and DFT/B3LYP (6-31++G(d,p)) calculations, in comparison with those in proline mono peptide [6–8,12].

Bond/angle/dihedral angle	Conf. anal.	DFT	References[a]		
		6-31G++(d,p)	[6]	[12]	[7]
N2—C12 (N—C^{α})	1.480	1.480	1.4520	1.469	1.469
C12—C9(C^{α}—C^{β})	1.549	1.552	1.5514	1.556	1.565
C9—C6(C^{β}—C^{γ})	1.535	1.538	1.5318	1.542	1.544
C6—C3(C^{γ}—Cδ)	1.532	1.532	1.5238	1.538	1.531
N2—C3(Cδ—N)	1.476	1.477		1.474	
H1—N2(N—H)	1.013	1.014	0.9976	1.013	1.022
C6—C3—N2(C^{γ}—Cδ—N)	103.44	103.173		104.41	
C9—C6—C3(C^{β}—C^{γ}—Cδ)	102.355	102.503	102.32	103.30	102.2
C6—C9—C12(C^{α}—C^{β}—C^{γ})	103.148	103.711	103.39	103.74	103.9
N2—C12—C9(N—C^{α}—C^{β})	105.530	105.356	105.76	105.58	
C3—N2—C12(Cδ—N—C^{α})	109.476	109.636		107.66	
N2—C12—C14—O15	177.958	175.866	174.50		
N2—C12—C9—C6(N—C^{α}—C^{β}—C^{γ})	21.943	18.747	−13.45		
C3—C6—C9—C12(Cδ—C^{γ}—C^{β}—C^{α})	−37.189	−35.406	32.97		−27.4
C6—C9—C12—C14(C^{γ}—C^{β}—C^{α}—C^{14})	−100.366	−104.083			98.6
C9—C12—N2—C3(χ^{o})	2.452	5.939	2[b]	3.6[c]	
C6—C9—C12—N2(χ^{1})	21.943	18.747		20.8[c]	
C3—C6—C9—C12(χ^{2})	−37.189	−35.406		−36.5[c]	
N2—C3—C6—C9(χ^{3})	38.924	39.040		38.4[c]	
C12—N2—C3—C6(χ^{4})	−25.969	−28.319		−26.6[c]	

[a] Taken from Refs. [6,12,7], except where indicated with "b" and "c".
[b] Taken from Ref. [13].
[c] Taken from Ref. [8].

that proline side chains adopt two different conformational states usually denoted as up (upPro) and down. UpPro and downPro can be identified by considering the distribution of proline side chain dihedral angles. In particular, upPro is characterized by negative values of χ^1 and χ^3 and positive values of χ^2 and χ^4, whereas downPro is characterized by positive values of χ^1 and χ^3 and negative values of χ^2 and χ^4 [23]. As seen in Table 2, in Pro–Tyr dipeptide, pyrrolidine ring structure is almost the same to that of mono proline. On the other hand results indicate that downPro conformation is adopted in Pro–Tyr dipeptide.

The calculated wavenumbers and the total energy distribution of the vibrational modes of monomeric and dimeric forms of Pro–Tyr dipeptide are given in Table 3 in comparison with the experimental IR and Raman spectra of solid phase of dipeptide. Experimental Raman and IR spectra for solid Pro–Tyr dipeptide are shown in Fig. 2.

3.1. CH_2 and CH group vibrations

Antisymmetric ($\upsilon_{as}CH_2$) and symmetric stretching (υ_sCH_2) vibrations of methylene group appear around 3000 ± 50 cm^{-1} and 2965 ± 30 cm^{-1} respectively. [24,25] For Pro–Tyr dipeptide, the $\upsilon_{as}CH_2$ vibrational wavenumbers are calculated at 2992 cm^{-1}, 2973 cm^{-1} and 2937 cm^{-1} for proline (see Table 3), and at 2965 cm^{-1} for tyrosine. The observed bands at 2993, 2939 cm^{-1} are assigned to $\upsilon_{as}CH_2$ mode of proline and the 2957 cm^{-1} band to $\upsilon_{as}CH_2$ mode of tyrosine in the Raman spectrum of solid Pro–Tyr dipeptide. These bands were observed at 3000 cm^{-1} and 2983 cm^{-1} in the Raman spectrum of mono L-proline [26], and at 2963 cm^{-1} in the IR spectrum of Ar matrix of L-tyrosine [1].

The CH_2 symmetric stretching wavenumbers (υ_sCH_2) of proline, in Pro–Tyr dipeptide were calculated at 2926 cm^{-1}, 2921 cm^{-1} and 2845 cm^{-1}, and observed at 2933 cm^{-1} and 2878 cm^{-1} in the Raman spectrum. These bands were observed at 2956, 2938 cm^{-1} in IR and 2950, 2938, 2900 cm^{-1} in Raman spectra of L-proline monopeptide [26]. The CH_2 symmetric stretching mode of tyrosine was calculated at 2908 cm^{-1} and observed at 2907 cm^{-1} in Raman spectrum of dipeptide, as a weak intense band.

Tyrosine has also aromatic CH stretching vibrations. The aromatic CH stretching modes ($\upsilon_{CH\ tyr\ (ring)}$) of Pro–Tyr dipeptide were calculated at 3066, 3042, 3034, and 3023 cm^{-1}. For tyrosine mono peptide, these bands were observed at 3046, 3036, and 3019 cm^{-1} [1], in the IR spectrum of Ar matrix. We assigned 3060 cm^{-1}, 3036 cm^{-1}, and 3026 cm^{-1} Raman bands, and 3071 cm^{-1}, 3047 cm^{-1}, 3019 cm^{-1} IR bands to CH stretching vibrations of tyrosine ring in Pro–Tyr dipeptide.

The CH_2 scissoring (δCH_2), wagging (ωCH_2), twisting (τCH_2) and rocking (ρCH_2) vibrations of proline appear in the 1455 ± 55 cm^{-1}, 1350 ± 85 cm^{-1}, 1290 ± 45 cm^{-1} and 890 ± 55 cm^{-1} regions respectively [26]. In the IR spectrum of solid spectrum of Pro–Tyr dipeptide, we observed three medium intense bands at 1490, 1472 and 1457 cm^{-1} which can be attributable to the CH_2 scissoring mode (δCH_2) of proline. The CH_2 scissoring (δCH_2), vibrations of proline, in dipeptide, were calculated at 1496, 1474 and 1464 cm^{-1}. We observed a single band at 1456 cm^{-1} in the Raman spectrum of dipeptide corresponding to δCH_2 mode of proline. The scissoring (δCH_2) vibration of tyrosine appears at 1448 cm^{-1} and 1449 cm^{-1} in IR and Raman spectra of dipeptide, respectively. Calculated wavenumber of this mode is 1459 cm^{-1}. For L-tyrosine mono peptide this band is observed at 1447 cm^{-1} in the IR spectrum of Ar matrix [1].

The CH_2 wagging modes are observed at 1355, and 1281 cm^{-1} as medium intense bands in the Raman and, at 1357 and 1293 cm^{-1} in IR spectra of solid Pro–Tyr dipeptide. Corresponding calculated wavenumbers are 1348, 1320 and 1294 cm^{-1}. For L-proline monopeptide, these modes were calculated at 1363, 1351 and 1342 cm^{-1} by HF Theory [26]. Our results are in agreement with those L-proline monopeptide.

The CH_2 twisting modes (τCH_2) of proline in Pro–Tyr dipeptide were calculated at 1243, 1216 and 1176 cm^{-1}. These modes are assigned to 1204 cm^{-1} strong and 1174 cm^{-1} weak intense bands, in the experimental Raman, and 1174 cm^{-1} medium intense band in the IR spectra of dipeptide.

The CH_2 rocking (ρCH_2) vibrations of proline in dipeptide are calculated at 945, 871 and 836 cm^{-1}. We assigned the 945 cm^{-1} and 866 cm^{-1} Raman bands and the 859 cm^{-1} IR band to these modes.

Table 3
Calculated and experimental wavenumbers (cm^{-1}) and the total energy distribution of the vibrational modes of the mono Pro–Tyr and calculated wavenumbers of its dimer.

	IR	Raman	Monomer		Dimer	
			6-31++G(d,p)	6-31G(d,p)	6-31G(d,p)	
	υ_{exp}	υ_{exp}	$*\upsilon$	$*\upsilon$	$*\upsilon$	TED[†] of mono Pro–Tyr 6-31G++(d,p)
1 $\upsilon_{OH\ tyr}$			3657	3582	3650;3650	$\upsilon_{OH}(100)$
2 $\upsilon_{OH(COOH)}$			3581	3515	2979;2864	$\upsilon_{OH}(100)$
3 $\upsilon_{NH\ (pro)}$			3411	3385	3409;3408	$\upsilon_{NH}(99)$
4 $\upsilon_{NH(peptid)}$	3318 s	3317 m	3381	3378	3393;3393	$\upsilon_{NH}(99)$
5 $\upsilon_{CH\ tyr\ (ring)}$	3071 w	3060 m	3066	3070	3067;3067	$\upsilon_{CH}(99)$
6 $\upsilon_{CH\ tyr\ (ring)}$			3042	3049	3051;3051	$\upsilon_{CH}(98)$
7 $\upsilon_{CH\ tyr\ (ring)}$	3047 w	3036 vw	3034	3039	3033;3033	$\upsilon_{CH}(99)$
8 $\upsilon_{CH\ tyr\ (ring)}$	3019 w	3026 vw	3023	3024	3024;3024	$\upsilon_{CH}(99)$
9 $\upsilon_{CH\ pro\ (asim)}$		2993 s	2992	3001	2999;2999	$\upsilon_{CH}(96)$
10 $\upsilon_{CH\ pro\ (asim)}$			2973	2982	2982;2982	$\upsilon_{CH}(98)$
11 $\upsilon_{CH2\ tyr\ (asim)}$	2965 m	2957 s	2965	2968	2962;2960	$\upsilon_{CH}(100)$
12 $\upsilon_{CH2\ tyr\ (asim)}$			2949	2950	2947;2947	$\upsilon_{CH}(100)$
13 $\upsilon_{CH\ pro\ (asim)}$		2939 vw	2937	2942	2939;2939	$\upsilon_{CH}(97)$
14 $\upsilon_{CH\ pro\ (sim)}$		2933 vw	2926	2932	2929;2929	$\upsilon_{CH}(98)$
15 $\upsilon_{CH\ pro\ (sim)}$			2921	2928	2926;2926	$\upsilon_{CH}(99)$
16 $\upsilon_{CH2tyr\ (sim)}$		2907 vw	2908	2914	2907;2907	$\upsilon_{CH}(99)$
17 $\upsilon_{CH(pro)}$		2902 vw	2907	2912	2911;2911	$\upsilon_{CH}(97)$
18 $\upsilon_{CH\ pro\ (sim)}$		2878 m	2845	2853	2848;2848	$\upsilon_{CH}(97)$
19 $\upsilon_{O=C\ (COOH)}$	1650 s	1661 m	1735	1762	1723;1665	$\upsilon_{OC}(85)$
20 $\upsilon_{C=O(pept.-amid\ I)}$			1700	1714	1713;1709	$\upsilon_{NC}(5) + \upsilon_{OC}(82)$
21 $\upsilon_{CC(tyr-ring)}$	1623 m	1612 s	1626	1622	1620;1620	$\upsilon_{CC}(64) + \delta_{HCC}(15)$
22 $\upsilon_{CC\ (tyr-ring)}$	1594 w	1594 m	1602	1597	1593;1593	$\upsilon_{CC}\ 68) + \delta_{COH}(5)$
23 $\delta_{CH\ ring} + \upsilon_{CCring}$			1517	1515	1511;1511	$\upsilon_{NC}(5) + \upsilon_{OC}(5) + \upsilon_{CC}(23) + \delta_{HCC}(40) + \delta_{HNC}(10)$
24 $\delta_{NH(pept.-amid\ II)}$	1516 s	1515 w	1510	1510	1500;1499	$\upsilon_{NC}(22) + \delta_{HNC}(33)$
25 $\delta_{HCHpro(scis)}$	1490 m		1496	1498	1488;1488	$\delta_{HCH}(25) + \Gamma_{HCNH}(9) + \Gamma_{HCCH}(17) + \Gamma_{CCCH}(9) + \Gamma_{HCNC}(10)$
26 $\delta_{HCHpro(scis)}$	1472 m		1474	1480	1469;1469	$\delta_{HCH}(25) + \Gamma_{HCCH}(47) + \Gamma_{NCCH}(8)$
27 $\delta_{HCHpro(scis)}$	1457 m	1456 m	1464	1470	1458;1458	$\delta_{HCH}(28) + \Gamma_{HCCH}(35) + \Gamma_{NCCH}(8) + \Gamma_{CCCH}(9)$
28 $\delta_{HCH\ tyr(scis)}$	1448 m	1449 m	1459	1469	1452;1452	$\delta_{HCH}(28) + \delta_{HCC}(5) + \Gamma_{NCCH}(13) + \Gamma_{CCCH}(42)$
29 $\upsilon_{CCtyrring} + \delta_{CH\ ring}$	1424 w	1422w	1438	1438	1432;1431	$\upsilon_{CC}(32) + \delta_{COH}(7) + \delta_{CCH}(29)$
30 $\delta_{CNH(pro)}$	1419 w	1403vw	1408	1406	1393;1393	$\delta_{CNH}(42) + \Gamma_{HCNC}(16) + \Gamma_{HCNH}(14)$
31 $\upsilon_{CC} + \delta_{COH}$	1377 m	1376vw	1365	1362	1343;1342	$\upsilon_{CC}(10) + \upsilon_{OC}(9) + \delta_{HNC}(7) + \delta_{HCC}(10) + \delta_{OCO}(10) + \delta_{COH}(7) + \Gamma_{HCCH}(15) + \Gamma_{CCCH}(7)$
32 $\delta_{HCCpro\ (wag.)}$	1357 m	1355 m	1348	1351	1339;1338	$\delta_{HNC}(17) + \delta_{HCC}(13) + \Gamma_{HCCH}(9) + \Gamma_{CCCH}(15) + \Gamma_{HCNC}(6) + \Gamma_{HCNH}(6)$
33 $\upsilon_{CCtyrring} + \delta_{HCCwag}$	1340 w		1341	1341	1334;1334	$\upsilon_{CC}(54) + \delta_{HCC}(16) + \delta_{COH}(7)$
34 $\delta_{HCC\ (tyr\ in-plane)}$	1324 w	1324 vw	1334	1338	1331;1331	$\delta_{HCC}(65) + \delta_{COH}(11)$
35 $\delta_{HCCpro(wag.)}$		1313 vw	1320	1324	1315;1315	$\delta_{HCC}(32) + \Gamma_{HCCH}(23) + \Gamma_{HCNC}(10)$
36 $\delta_{HCC(tyr\ in-plane)}$			1311	1313	1300;1300	$\upsilon_{CC}(12) + \delta_{HCC}(42)$
37 δ_{COH}		1303 w	1302	1305	1470;1289	$\upsilon_{OC}(9) + \delta_{HCC}(20) + \delta_{OCO}(5) + \delta_{COH}(20) + \Gamma_{OCCH}(9)$
38 $\delta_{HCC(pro)}$			1297	1296	1286;1286	$\delta_{HCC}(24) + \Gamma_{HCCH}(10) + \Gamma_{CCCH}(5) + \Gamma_{HCNC}(7) + \Gamma_{HCNH}(12)$
39 $\delta_{HCCpro\ (wag.)}$	1293 w	1281 m	1294	1291	1282;1282	$\delta_{HCC}(33) + \Gamma_{HCCH}(26)$
40 $\upsilon_{OC\ (tyr)}$	1268 w	1265 vw	1257	1265	1265;1264	$\upsilon_{CC}(21) + \upsilon_{OC}(50) + \delta_{HCC}(11)$
41 $\delta_{HCC} + \delta_{COH}$	1232 w	1232 m	1253	1250	1237;1236	$\delta_{COH}(17) + \delta_{HCC}(30) + \Gamma_{HCNC}(5) + \Gamma_{HCNH}(5)$
42 $\delta_{HCCpro\ (twist)}$			1243	1241	1232;1232	$\delta_{HCN}(5) + \delta_{HCC}(23) + \Gamma_{HCNH}(5) + \Gamma_{OCCH}(6)$
43 $\upsilon_{NC(pept.-amid\ III)}$	1228 w		1227	1217	1197;1197	$\upsilon_{CC}(8) + \upsilon_{NC}(12) + \delta_{HNC}(24)$
44 $\delta_{HCCpro\ (twist)}$		1204 s	1216	1212	1210;1210	$\upsilon_{NC}(5) + \delta_{HNC}(8) + \delta_{HCC}(13)$
45 $\upsilon_{CC\ tyr}$	1205 vs	1200 vs	1201	1195	1191;1191	$\upsilon_{CC}(60) + \delta_{HCC}(9)$
46 $\delta_{HCN} + \upsilon_{NC\ peptid}$	1189 w		1195	1193	1186;1186	$\upsilon_{NC}(13) + \delta_{HCC}(12) + \delta_{HCN}(14)$
47 $\delta_{HCCpro\ (twist)}$	1174 m	1174 w	1176	1174	1169;1169	$\upsilon_{CC}(10) + \delta_{HCC}(26) + \Gamma_{HCCH}(6)$
48 $\delta_{CH-ring-tyr}$			1170	1173	1164;1164	$\upsilon_{CC}(15) + \delta_{HCC}(77)$
49 $\delta_{COH\ (tyr)}$			1162	1168	1159;1159	$\upsilon_{CC}(18) + \delta_{HCC}(14) + \delta_{COH}(59)$
50 δ_{HNC}	1156w		1150	1146	1138;1138	$\upsilon_{NC}(11) + \delta_{HNC}(19) + \Gamma_{HCCH}(7) + \Gamma_{CCCH}(8)$
51 $\upsilon_{OC} + \delta_{COH}$	1136w		1138	1142	1115;1115	$\upsilon_{NC}(9) + \upsilon_{OC}(19) + \delta_{COH}(17)$
52 υ_{NC}	1113 m	1111 w	1107	1107		$\upsilon_{NC}(28) + \upsilon_{OC}(17) + \delta_{COH}(8)$
53 $\upsilon_{CCtyrring} + \delta_{CH\ ring}$			1104	1101	1098;1098	$\upsilon_{CC}(19) + \delta_{HCC}(41)$
54 $\upsilon_{NC\ (N-C\ )}$		1093 w	1097	1096	1093;1093	$\upsilon_{NC}(40) + \upsilon_{OC}(6)$
55 δ_{HCCpro}		1078 w	1071	1067	1063;1063	$\upsilon_{NC}(23) + \delta_{HCC}(10) + \Gamma_{CCCH}(15)$
56 $\upsilon_{CC(pro-ring)}$	1030 m	1040 w	1036	1028	1025;1025	$\upsilon_{NC}(6) + \upsilon_{CC}(41) + \delta_{HCC}(7)$
57 $\upsilon_{CC(tyr)}$		1025 m	1015	1004	1001;1000	$\upsilon_{CC}(26) + \delta_{HCC}(8)$
58 $\upsilon_{CCtyrring} + \delta_{ring}$		994 w	1005	999	996;996	$\upsilon_{CC}(31) + \delta_{HCC}(31) + \delta_{CCC}(32)$
59 $\upsilon_{CC(pro-ring)}$	963 m		963	963	967;963	$\upsilon_{NC}(21) + \upsilon_{CC}(41)$
60 $\delta_{HCCpro\ (rock.)}$			945	942	946;939	$\upsilon_{CC}(8) + \Gamma_{HCCH}(23) + \Gamma_{CCCH}(18)$
61 $\gamma_{(C-H\ ring-tyr)}$			943	931	936;934	$\upsilon_{NC}(5) + \upsilon_{CC}(15) + \Gamma_{HCCH}(16) + \Gamma_{CCCH}(8)$
62 $\gamma_{(C-H\ ring-tyr)}$	924 m	937 m	934	920	924;924	$\upsilon_{CC}(10) + \Gamma_{HCCH}(20) + \Gamma_{CCCH}(22)$
63 $\gamma_{(C-H\ ring-tyr)}$			917	908	907;907	$\upsilon_{NC}(7) + \upsilon_{CC}(22) + \Gamma_{HCCH}(13)$
64 $\upsilon_{CC(pro-ring)}$			908	899	899;899	$\upsilon_{NC}(6) + \upsilon_{CC}(27)$
65 $\upsilon_{CCpro\ (ring-breath)}$		912 m	892	887	885;885	$\upsilon_{NC}(22) + \upsilon_{CC}(40)$
66 $\delta_{HCCpro\ (rock)}$	859 m	866 m	871	866	865;865	$\upsilon_{NC}(8) + \upsilon_{CC}(15) + \delta_{HCC}(12) + \delta_{CCC}(5)$
67 υ_{NC}		848 w	860	862	861;861	$\upsilon_{NC}(10) + \upsilon_{CC}(7) + \delta_{HCC}(5)$
68 $\upsilon_{CC\ tyr\ (ring-breath)}$		841 s	841	838	839;838	$\upsilon_{CC}(43) + \upsilon_{OC}(6)$
69 $\delta_{CNHpro\ (rock.)}$			836	835	831;831	$\upsilon_{CC}(6) + \delta_{CNH}(9) + \Gamma_{CNCH}(9)$
70 $\gamma_{(C-H\ ring-tyr)}$	827 s	824 vs	828	825	826;826	$\upsilon_{CC}(13) + \delta_{OCN}(6)$
71 $\gamma_{(C-H\ ring-tyr)}$		805 vw	815	808	808;808	$\Gamma_{OCCH}(17) + \Gamma_{CCCH}(49)$
72 $\gamma_{(C-H\ ring-tyr)}$			798	787	789;788	$\Gamma_{OCCH}(22) + \Gamma_{CCCH}(63)$

(*continued on next page*)

Table 3 (*continued*)

	IR	Raman	Monomer		Dimer	
			6-31++G(d,p)	6-31G(d,p)	6-31G(d,p)	
	υ_{exp}	υ_{exp}	$*\upsilon$	$*\upsilon$	$*\upsilon$	TED† of mono Pro–Tyr 6-31G++(d,p)
73 $\delta_{ring\text{-}tyr}$	767 w	763 vw	775	771	780;776	$\upsilon_{CC}(31) + \upsilon_{OC}(12) + \delta_{CCC}(10)$
74 $\delta_{C=O(pept.\text{-}amid\ IV)}$	739 s	739 vw	747	739	739;739	$\Gamma_{OCCC}(5) + \Gamma_{OCCH}(5) + \Gamma_{OCNH}(16) + \Gamma_{NCCC}(5) + \Gamma_{NCCN}(6)$
75 $\Gamma_{CCCCtyr}$	718 s	719 m	717	714	704;703	$\delta_{CCC}(5) + \Gamma_{OCCC}(6) + \Gamma_{CCCC}(22) + \Gamma_{COOH}(15) + \Gamma_{OCCN}(5)$
76 $\Gamma_{ring\text{-}tyr}$	705 m		693	691	696;685	$\upsilon_{CC}(12) + \Gamma_{COOH}(11) + \Gamma_{CCCC}(26)$
77 Γ_{NCCH}	668 s	662 m	676	661	663;661	$\delta_{OCN}(5) + \Gamma_{NCCH}(43) + \Gamma_{OCNH}(18)$
78 $\delta_{OCO\ (COOH)}$	652 w		642	636	670;660	$\upsilon_{OC}(14) + \delta_{CCO}(19) + \delta_{OCO}(27) + \delta_{COH}(5)$
79 $\delta_{ring\text{-}tyr}$		641 m	641	634	635;635	$\upsilon_{CC}(7) + \delta_{HCC}(14) + \delta_{OCC}(7) + \delta_{CCC}(49)$
80 $\delta_{pro\text{-}ring}$	603 m	596 vw	610	600	600;599	$\upsilon_{CC}(10) + \delta_{OCN}(5) + \delta_{CNC}(8) + \Gamma_{HCNH}(6) + \Gamma_{CCNH}(16)$
81 Γ_{CCOH}			583	592	986	$\Gamma_{CCOH}(50) + \Gamma_{COOH}(24)$
82 $\delta_{pro\text{-}ring}$			575	569	580;574	$\upsilon_{NC}(5) + \delta_{CCC}(5) + \delta_{NCC}(7) + \delta_{OCC}(5) + \Gamma_{OCCN}(6)$
83 $\delta_{pro\text{-}ring}$	560 m	560 vw	555	551	554;552	$\delta_{CCC}(12) + \delta_{NCC}(18) + \delta_{OCC}(5) + \Gamma_{CCNH}(12)$
84 $\gamma_{(C-H\ ring\text{-}tyr)}$	525 m		533	533	533;533	$\delta_{CCC}(10) + \Gamma_{CCCH}(28) + \Gamma_{CCCC}(6)$
85 $\gamma_{(C-H\ ring\text{-}tyr)}$	488 m	490 w	488	486	494;488	$\delta_{CCC}(8) + \Gamma_{CCCH}(16) + \Gamma_{CCCC}(8)$
86 δ_{OCC}			472	467	481;478	$\upsilon_{CC}(14) + \delta_{CCC}(7) + \delta_{OCO}(9) + \delta_{OCC}(18)$
87 δ_{OCC}	459 w	457 m	434	433	448;440	$\upsilon_{CC}(9) + \delta_{NCC}(9) + \delta_{OCC}(26)$
88 $\delta_{OCC(tyr)}$		416 vw	419	416	428;423	$\delta_{CCC}(5) + \delta_{OCC}(34)$
89 $\Gamma_{ring\text{-}tyr}$			413	410	410;410	$\delta_{CCC}(5) + \delta_{OCC}(20) + \Gamma_{CCCO}(5) + \Gamma_{CCCC}(27)$
90 $\Gamma_{ring\text{-}tyr}$		392 vw	412	408	408;408	$\delta_{NCC}(6) + \Gamma_{CCCO}(5) + \Gamma_{OCCN}(5) + \Gamma_{CCCC}(29)$
91 δ_{NCC}		360 vw	342	353	352;348	$\delta_{NCC}(15) + \Gamma_{CCCC}(8) + \Gamma_{CCCO}(11)$
92 $\Gamma_{CCOH\ (tyr)}$		333 vw	329	342	342;341	$\Gamma_{CCOH}(97)$
93 δ_{CCC}		314 w	312	310	306;305	$\delta_{OCC}(21) + \delta_{CCC}(28) + \Gamma_{CCNH}(9)$
94 δ_{CCC}			302	302	332;322	$\delta_{OCC}(6) + \delta_{CCC}(19) + \delta_{CNC}(7) + \Gamma_{CCCO}(7)$
95 $\gamma_{pro\text{-}ring}$			273	275	293;287	$\upsilon_{CC}(10) + \delta_{CCC}(5) + \Gamma_{CCCH}(13) + \Gamma_{CCCC}(5) + \Gamma_{HCCN}(7)$
96 $\gamma_{pro\text{-}ring\ +\ \delta OCC}$		266 vw	260	257	275;270	$\upsilon_{NC}(5) + \upsilon_{CC}(5) + \delta_{NCC}(16) + \delta_{OCC}(25)$
97 $\gamma_{pro\text{-}ring\ +\ \delta OCC}$		230 vw	214	212	222;220	$\delta_{CCC}(10) + \delta_{OCC}(25) + \Gamma_{HCCN}(12) + \Gamma_{CCCN}(12) + \Gamma_{CCCH}(7)$
98 δ_{CCC}			185	180	197;185	$\upsilon_{CC}(13) + \delta_{CCN}(5) + \delta_{CCC}(18) + \Gamma_{CCCN}(5) + \Gamma_{CCCO}(10)$
99 δ_{CCC}			134	134	159;159	$\delta_{CCC}(22) + \delta_{CCN}(5) + \Gamma_{CCCN}(4) + \Gamma_{CCCO}(11) + \Gamma_{CCCC}(6)$
100 $\delta_{CCN(pro)}$			122	122	141;135	$\delta_{CCN}(41) + \delta_{OCN}(5) + \delta_{CNH}(7) + \Gamma_{HCCN}(10) + \Gamma_{CCCN}(7) + \Gamma_{CCCO}(10)$
101 Γ_{CCCN}			76	75	115;101	$\delta_{CCC}(12) + \Gamma_{CCCN}(19) + \Gamma_{CNCO}(7) + \Gamma_{CCCH}(10) + \Gamma_{CCCC}(15)$
102 Γ_{CCCH}			61	61	64;63	$\delta_{CCC}(5) + \Gamma_{CCCC}(21) + \Gamma_{CCCH}(30) + \Gamma_{CCCN}(7) + \Gamma_{OCCH}(4) + \Gamma_{CNCO}(6) + \Gamma_{HCNH}(5)$
103 Γ_{NCCC}			56	55	64;92	$\Gamma_{CCCO}(7) + \Gamma_{NCCN}(14) + \Gamma_{NCCC}(30) + \Gamma_{NCCH}(22)$
104 Γ_{CCCH}			52	51	57;56;29	$\Gamma_{CCCH}(16) + \Gamma_{CCCC}(16) + \Gamma_{CCNH}(8) + \Gamma_{NCCC}(6) + \Gamma_{NCCO}(14)$
105 Γ_{CCOC}			41	43	79;52	$\Gamma_{OCCN}(32) + \Gamma_{OCCH}(12) + \Gamma_{OCCC}(25)$
106 $\Gamma_{CCCC(tyr)}$			28	30	34;31	$\Gamma_{CCCC}(40) + \Gamma_{CCCH}(37)$
107 Γ_{CCNC}			24	18	39;36	$\Gamma_{CCNH}(30) + \Gamma_{CCNC}(65)$
108 Γ_{CCNC}			21	12	23;22;18	$\Gamma_{CCNH}(25) + \Gamma_{CCNC}(26) + \Gamma_{CCCC}(10) + \Gamma_{OCCN}(13) + \Gamma_{HCNH}(8)$

The wavenumbers under 1800 cm^{-1}, were scaled either with 0.967 (for B3LYP/6-31G(d,p)) or 0.977 (for B3LYP/6-31++G(d,p)), and for over 1800 cm^{-1} the scale factor 0.955 were used for both B3LYP/6-31G(d,p), B3LYP/6-31++G(d,p) levels of theory.

† Only contributions >%5 are listed.

3.2. Carboxyl group vibrations

The C═O stretching vibrations gives rise to a strong band in the region 1660–1730 cm^{-1} [24,26,27]. In this work, the C═O stretching ($\upsilon_{C=O\ (COOH)}$) wavenumber was calculated at 1735 cm^{-1} for monomeric and 1723, 1665 cm^{-1} for dimeric forms of Pro–Tyr dipeptide. As seen in Fig. 2, this mode is observed at 1661 cm^{-1} as medium intense band in the Raman and at 1650 cm^{-1} as strong intense band in the IR spectra of solid Pro–Tyr. Rippon et al. [28] was observed this mode at 1643 cm^{-1} and 1645 cm^{-1} in the Raman and IR spectra of proline mono peptide respectively.

The OH in-plane deformation, coupled to the C—O stretching vibration, is expected in the region 1390 ± 55 cm^{-1} [26]. This mode is observed at 1377 cm^{-1} as a medium intense band and at 1376 cm^{-1} as a very weak intense band in the IR and Raman spectra of solid Pro–Tyr dipeptide, respectively. The HCC (δ_{HCC}) bending vibration, coupled to the OH in-plane deformation, is observed at 1232 cm^{-1} both in Raman and IR spectra of solid Pro–Tyr dipeptide. The C═O out-of plane bending vibrations are observed in the range 595 ± 85 cm^{-1} [26]. For this mode, 642 cm^{-1} wavenumber is calculated for monomeric and, 670 and 660 cm^{-1} wavenumbers are calculated for dimeric forms of dipeptide. The band observed at 652 cm^{-1} in the IR spectrum of solid Pro–Tyr dipeptide is attributable to this mode (see Table 3).

3.3. Peptide vibrations

The υ_{NH} peptide stretching mode is calculated at 3411 cm^{-1}, 3381 cm^{-1} for monomeric and 3409 cm^{-1} and 3393 cm^{-1} for dimeric forms of Pro–Tyr dipeptide, respectively, and is observed at 3318 cm^{-1} and 3317 cm^{-1} in the IR and Raman spectra of solid Pro–Tyr dipeptide, respectively.

The amide I band, $\upsilon_{C=O(peptid)}$, was calculated at 1693 cm^{-1} by Koleva et al. [29] for tyrosine monopeptide and our calculations resulted 1700 cm^{-1} wavenumber for the monomeric and 1709, 1713 cm^{-1} for the dimeric forms of Pro–Tyr dipeptide. The amide II ($\delta_{NH(peptid)}$) vibrational wavenumber is calculated at 1510 cm^{-1} for monomeric form and at 1500 cm^{-1} for dimeric form of Pro–Tyr dipeptide. The 1516 cm^{-1} and 1515 cm^{-1} bands observed in the IR and Raman spectra of solid Pro–Tyr dipeptide, respectively, are assigned to the amide II vibrational mode. This mode was reported to be 1515 cm^{-1} for tyrosine monopeptide [29].

The amide III band, $\upsilon_{NC(peptide)}$ is observed at 1228 cm^{-1} in the IR spectrum of solid Pro–Tyr dipeptide and calculated at 1227 cm^{-1}. The HCN bending mode coupled with CN stretching vibration ($\delta_{HCN} + \upsilon_{NC\ peptid}$) is calculated at 1195 cm^{-1} and observed at 1189 cm^{-1} in the IR spectrum of dipeptide.

The band observed at 739 cm^{-1} in both IR and Raman spectra of the dipeptide is assigned to the amide IV (δC═O) mode. This mode

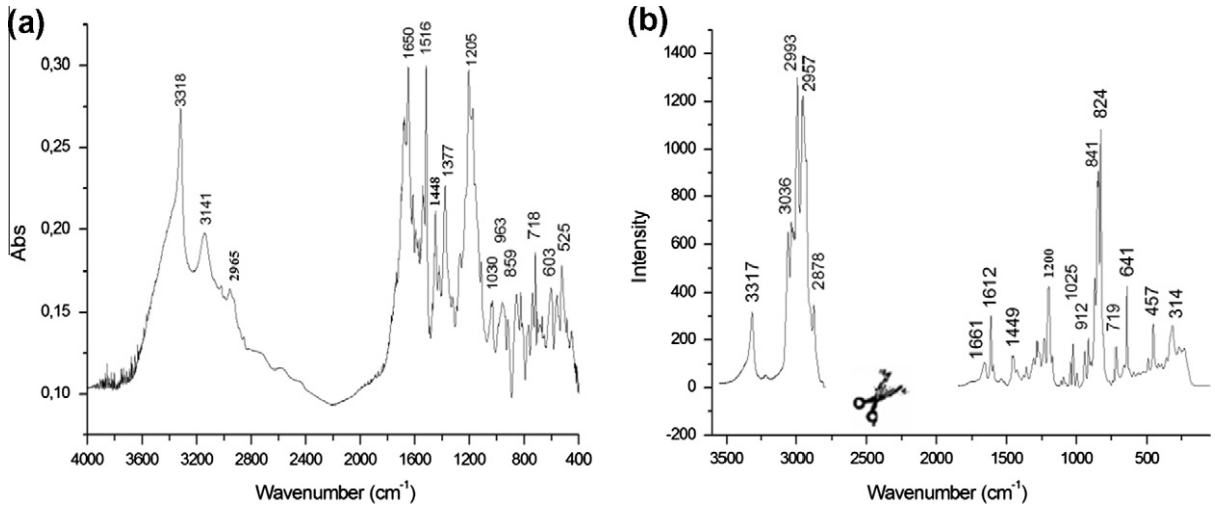

Fig. 2. FT-IR (a) and micro Raman spectra (b) of solid Pro–Tyr dipeptide.

was observed at 748 cm^{-1} and 763 cm^{-1} for H–Val–Tyr–OH and H–Tyr–Ala–OH dipeptide respectively [29].

3.4. Ring vibrations

For L-proline monopeptide the ring stretching vibrations were observed at 914, 983 and 1000 cm^{-1} by Rippon et al. [28]. On the other hand Podstawka et al. [30] were reported 1090 cm^{-1} (IR), 1083 cm^{-1} (R), 1025 cm^{-1} (IR), 1023 cm^{-1} (R), 907 cm^{-1} (IR), 900 cm^{-1} (R), 866 cm^{-1} (IR) 880 cm^{-1} (R) cm^{-1} wavenumbers as experimental and 1083 cm^{-1}, 1016 cm^{-1}, 908 cm^{-1}, 898 cm^{-1}, 876 cm^{-1} as calculated (HF) wavenumbers of the ring stretching vibrations proline monopeptide [30]. For Pro–Tyr dipeptide, we calculated 1036 cm^{-1}, 963 cm^{-1}, 908 cm^{-1}, and 892 cm^{-1} wavenumbers as the ring stretching modes of proline. In the experimental vibrational spectra of solid Pro–Tyr dipeptide we only observed one Raman band at 912 cm^{-1}, attributable to the ring stretching mode of proline and assigned as ring breathing mode of proline.

The in-plane ring bending modes of proline of the investigated dipeptide are calculated at 610, 575 and 555 cm^{-1}. The bands, observed in the vibrational spectra of solid Pro–Tyr dipeptide, 603 cm^{-1} (IR), 596 cm^{-1} (R), 560 cm^{-1} (IR, R) are assigned to these vibrations.

The out-of-plane bending modes for L-proline monopeptide were reported at 289 cm^{-1} and 252 cm^{-1} [26]. Our calculated values for out-of-plane bending modes ($\gamma_{pro\text{-}ring}$) of proline in Pro–Tyr dipeptide are 273 cm^{-1}, 260 cm^{-1} and 214 cm^{-1}.

Tyrosine ring stretching modes are observed at 1623 cm^{-1} (IR), 1612 cm^{-1} (R) and 1594 cm^{-1} (R) in the vibrational spectra of solid Pro–Tyr dipeptide. The calculated values for these modes are 1626 cm^{-1} and 1602 cm^{-1}. For tyrosine monopeptide ring stretching modes are assigned at 1623 cm^{-1} and 1600 cm^{-1} [1].

The tyrosine ring stretching modes coupled with CH bending modes ($\delta_{CH\ ring} + \upsilon_{CCring}$ and $\upsilon_{CCtyrring} + \delta_{CH\ ring}$) were calculated at 1517 cm^{-1} and 1438 cm^{-1} respectively. Our result is in agreement with that of Rippon et al. [28].

The ring bending mode coupled with the ring stretching ($\upsilon_{CCtyr\text{-}ring} + \delta_{ring}$) was calculated at 1005 cm^{-1} and observed at 994 cm^{-1} (R). This mode was assigned at 1004 cm^{-1} in tyrosine monopeptide [1].

The strong band observed at 841 cm^{-1} in Raman spectrum of Pro–Tyr dipeptide is assigned to the ring breathing vibrations of tyrosine in agreement to [1]. This mode is also calculated at 841 cm^{-1} for monomeric form of Pro–Tyr dipeptide.

In accord with [1], the bands, observed at 767 cm^{-1} (IR) and 641 cm^{-1} (R), in the vibrational spectra of solid Pro–Tyr dipeptide are assigned to ring bending modes of tyrosine ($\delta_{ring\text{-}tyr}$). The calculated values for these modes are 775 cm^{-1}, 641 cm^{-1}, respectively.

4. Conclusion

In this study the structural characteristics of monomeric and dimeric forms of Pro–Tyr dipeptide were revealed. This investigation provides a rather satisfactory theoretical description of the dipeptide. Our calculations of the spatial structures of biologically active L-Pro–Tyr dipeptide demonstrated that the molecule had a limited set of the stable structures that are characterized by the folded backbone form. Intra-hydrogen bonding interaction of monomeric, and inter- and intra-hydrogen bonding interactions of dimeric forms of dipeptide are determined. Pro–Tyr dipeptide gives non-planar structure of the amide plane. Strong deviation of dihedral angle from 180° were occured due to H-bonding between amide plane hydrogen 17H and 36O (~2.60 Å) of carboxylic group of dipeptide. The determination of conformational possibilities of L-Pro–Tyr dipeptide may be useful as a base for synthesis of its more effective structural analogs.

Acknowledgment

This study was supported by the Research fund of Istanbul University (Project Numbers ONAP-2423, T/3171, UDP-7165 and UDP-7167).

References

[1] R. Ramaekers, J. Pajak, M. Rospenk, G. Maes, Spectrochim. Acta Part A 61 (2005) 1347.
[2] T.A. Gudasheva, N.I. Zaitseva, N.A. Bondarenko, I.E. Shcherbakova, L.S. Asmakova, G.G. Rozantsev, R.U. Ostrovskaya, T.A. Voronina, S.B. Seredenin, Pharm. Chem. J. 31 (1997) 574.
[3] I.H. Lee, S.M. Kim, W.S. Suh, Korean Chem. Soc. 9 (1988) 218.
[4] A.E. Ledesma, C.D. Contreras, H.E. Lanús, Brandan Silvia, in: XXII International Conference on Raman Spectroscopy. AIP Conference Proceedings, vol. 1267, 2010, pp. 1213.
[5] H. Takeuchi, N. Watanabe, Y. Satoh, I. Harada, J. Raman Spectrosc. 20 (1989) 233.
[6] M. Ramek, A.-M. Kelterer, S. Nikolic, Int. J. Quantum Chem. 65 (1997) 1033.
[7] S.G. Stepanian, I.D. Reva, E.D. Radchenko, L. Adamowicz, J. Phys. Chem. A 105 (2001) 10664.
[8] Y.K. Kang, J. Mol. Struct. (Theochem.) 675 (2004) 37.
[9] B. Maigret, D. Perahia, B. Pulman, J. Theor. Biol. 29 (1970) 275.

[10] H.A. Baldoni, A.M. Rodrigues, M.A. Zamora, G.N. Zamarbide, R.D. Enriz, O. Farkas, P. Csaszar, L.L. Torday, C.P. Sosa, I. Jakli, A. Perzel, J.Gy. Papp, M. Hollosi, I.G. Csizmadia, J. Mol. Struct. (Theochem.) 465 (1999) 79.
[11] I. Hudaky, H.A. Baldoni, A. Perczel, J. Mol. Struct. (Theochem.) 581 (2002) 233.
[12] E. Czinki, A.G. Csaszar, Chem. Eur. J. 9 (2003) 1008.
[13] W.D. Allen, E. Czinki, A.G. Csaszar, Chem. Eur. J. 10 (2004) 4512.
[14] N.M. Godjaev, I.S. Maksumov, L.I. Ismailova, J. Chem. Struct. (Russian) 24 (1983) 147.
[15] N. Ramachandran, Biopolymers 6 (1968) 1494.
[16] G.N. Ramachandran, C. Ramakrishnan, V. Sasisekharan, J. Mol. Biol. 7 (1963) 95.
[17] Gaussian 03, Revision C.02, M.J. Frisch, G.W. Trucks, H.B. Schlegel, G.E. Scuseria, M.A. Robb, J.R. Cheeseman, J.A. Montgomery Jr., T.Vreven, K.N. Kudin, J.C. Burant, J.M. Millam, S.S. Iyengar, J. Tomasi, V.Barone, B. Mennucci, M. Cossi, G. Scalmani, N. Rega, G.A. Petersson, H. Nakatsuji, M. Hada, M. Ehara, K. Toyota, R. Fukuda, J. Hasegawa, M. Ishida, T. Nakajima, Y. Honda, O. Kitao, H. Nakai, M. Klene, X. Li, J.E. Knox, H.P. Hratchian, J.B. Cross, V. Bakken, C. Adamo, J. Jaramillo, R. Gomperts, R.E. Stratmann, O. Yazyev, A.J. Austin, R. Cammi, C. Pomelli, J.W. Ochterski, P.Y. Ayala, K. Morokuma, G.A. Voth, P. Salvador, J.J. Dannenberg, V.G. Zakrzewski, S. Dapprich, A.D. Daniels, M.C. Strain, O. Farkas, D.K. Malick, A.D. Rabuck, K. Raghavachari, J.B. Foresman, J.V. Ortiz, Q. Cui, A.G. Baboul, S. Clifford, J. Cioslowski, B.B. Stefanov, G. Liu, A. Liashenko, P. Piskorz, I. Komaromi, R.L. Martin, D.J. Fox, T. Keith, M.A. Al-Laham, C.Y. Peng, A. Nanayakkara, M. Challacombe, P.M.W. Gill, B. Johnson, W. Chen, M.W. Wong, C. Gonzalez, J.A. Pople, Gaussian, Inc., Wallingford CT, 2004.
[18] PQS Version 3.1, Parallel Quantum Solutions, 2013 Green Acres Road, Suite A Fayetteville, Arkansas, 72703 USA.
[19] S. Kecel, A.E. Ozel, S. Akyuz, S. Celik, J. Spectrosc. Biomed. Appl. 24 (2010) 219.
[20] S. Mondal, D.S. Chowdhuri, S. Ghosh, A. Misra, S. Dalai, J. Mol. Struct. (Theochem.) 810 (2007) 81.
[21] S. Ghosh, S. Mondal, A. Misra, S. Dalai, J. Mol. Struct. (Theochem.) 805 (2007) 133.
[22] A.F. Ortega, Conformational Properties of Constrained Proline Analogues and Their Application in Nanobiology, Ph.D. Thesis, Department D'enginyeria Quimica, Universitat Politècnica De Catalunya, Barcelona, 2009.
[23] L. Vitagliano, R. Berisio, A. Mastrangelo, L. Mazzarella, A. Zagari, Protein Sci. 10 (2001) 2627.
[24] N.P.G. Roeges, A Guide to the Complete Interpretation of Infrared Spectra of Organic Structures, Wiley, New York, 1994.
[25] N.B. Colthup, L.H. Daly, S.E. Wiberly, Introduction to Infrared and Raman Spectroscopy, Academic Press, New York, 1975.
[26] Y.S. Mary, L. Ushakumari, B. Harıkumar, T.H. Varghese, Y.C. Panicker, J. Iran Chem. Soc. 6 (2008) 138.
[27] L. Padmaja, C. Ravikumar, C. James, V.S. Jayakumar, I. Joe, Spectrochim. Acta Part A 71 (2008) 252.
[28] W.B. Rippon, J.L. Koenig, A.G. Walton, J. Am. Chem. Soc. 92 (1970) 7455.
[29] B.B. Koleva, T.M. Kolev, M. Spiteller, Spectrochim. Acta Part A 68 (2007) 1187.
[30] E. Podstawka, Y. Ozaki, L.M. Proniewicz, Appl. Spectrosc. 58 (2004) 570.